How the camber and thickness positions affect the lift produced at different angles of attack
Mina Mikhail

Abstract

This study attempts to create a stall-resistant wing by changing the position of the airfoil's camber and thickness. Wing stalling occurs at high angles of attack when the airflow above the wing's surface detaches and becomes turbulent. Stalling causes a dramatic loss of lift, making it impossible for the wings to sustain the aircraft, which can be catastrophic in flight. Stalling characteristics place large restrictions on flight in terms of the minimum speeds of an aircraft and the maximum angle of attack that can be achieved. We investigated how the lift coefficients of an airfoil at different angles of attack are affected by changing camber and thickness positions to attempt to achieve better stalling characteristics. We tested five airfoils produced through three-dimensional printing, that differed solely in their camber and thickness positions, within a custom-made wind-tunnel. Our findings show that as the camber of the wing moves forward more lift is produced at any given angle of attack but there is a trade-off of a decreased stall angle, so the wing stalls sooner. Therefore, a stall resistant wing could be made by moving the camber and thickness position of a wing rearward, but this would sacrifice some lift. This could have implications for future airfoil designs.

Introduction

Air follows the curvature of an airfoil due to the Coanda effect which states that a fluid jet will adhere to the surface it moves over[1]. The higher the angle of deflection, the lower its tendency to adhere to the surface[1]. Thus, at slower aircraft speeds, and consequently higher angles of attack to produce an adequate amount of lift, the boundary layer separates from the airfoil[2]. A stall occurs when the wings no longer produce enough lift to keep the aircraft at a steady altitude[2].

The airfoil's upper surface plays an integral role in the production of lift, therefore airflow separation is catastrophic to lift production. Two of the accepted theories of lift are Bernoulli's equation: the airflow above a wing has a higher velocity due to its camber and therefore lower pressure, and Newton's third law of motion: an action has a re-action, thus air deflected downward by the upper and lower surfaces of a wing produces a lift force[3]. In the first theory, a stall prevents a pressure gradient from being created, and in the second, a wing loses one of its surfaces by which it produces lift.

There have been many attempts at creating a stall-resistant wing, including a pronounced curvature[4], a rough surface[5], and through numerical investigations including Navier-

Stokes equations[6]. This study aims to create a stall-resistant wing by moving the camber and thickness of the wing unusually far forward and rearward. Previous studies show that forward cambered wings may have promising stall-resistant characteristics in terms of high angles of attack having large lift coefficients[7,8].

Results

Five airfoils were developed in the final design. All airfoils were identified by their modified four-digit NACA number. The only NACA features that were altered between the airfoils were the maximum thickness and camber positions[9]. An airfoil's lift force in pounds was determined by:

$$Equation\ 1: L = C_l \times A \times 0.5 \times r \times V^2$$

assuming that C_l is the lift coefficient, A is the wing area in ft^2, r is density in $slugs/ft^3$, and V is the velocity in ft/s[10,11,12].

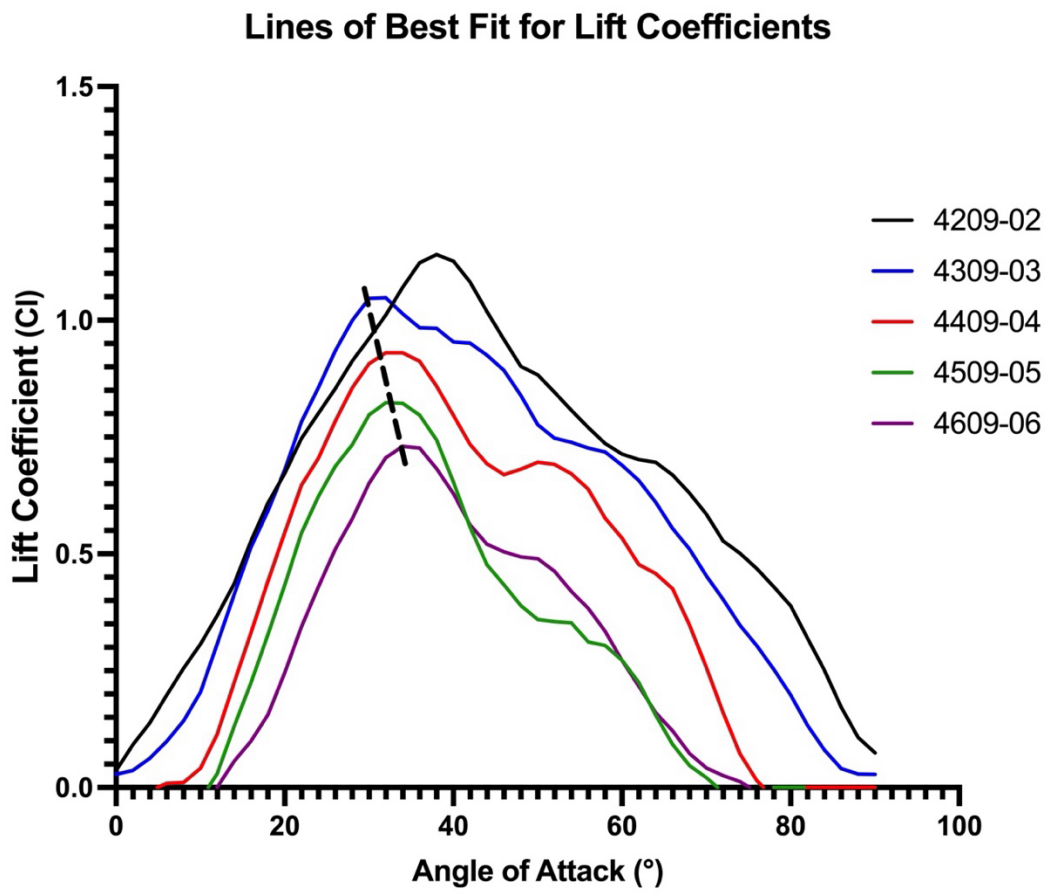

Figure 1: Effect of camber position on the lift produced at different angles of attack. The dashed line shows the trend in the stall angles.

Figure 1 shows that as the camber and thickness positions of the wing move forward, the wing produces higher lift at any given angle of attack and at the same time the stall (peak) angle of attack decreases with the exception of 4209-02. The dashed line shows the trend in stall angle, which highlights a decreasing trend from airfoil 4309-03 to airfoil 4609-06; only airfoil 4209-02 does not follow this pattern.

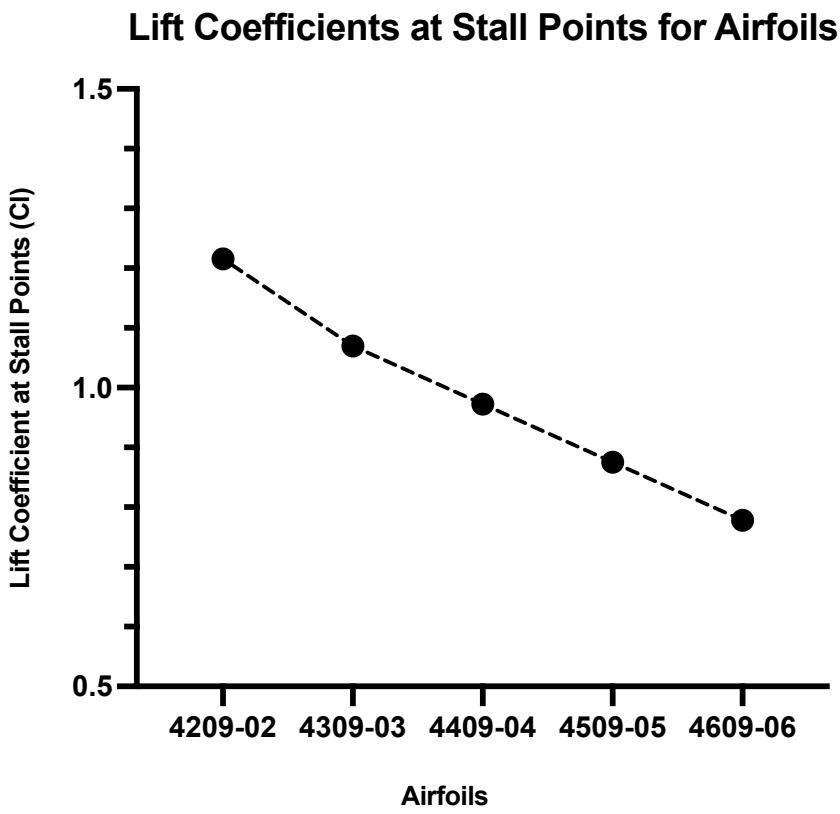

Figure 2: The peak lift coefficients for each airfoil.

The maximum lift coefficients for each airfoil are higher for forward cambered wings as seen in figure 2. Airfoil 4209-02 has the largest maximum lift coefficient while airfoil 4609-06 has the smallest maximum lift coefficient.

Statistical Analysis of the Airfoils

Paired t-test analysis between the different airfoils shows significant differences for each comparison except for airfoils 4409-04 and 4609-06. This last comparison shows a higher rate than our accepted error rate cutoff (5%) meaning the difference may not be real.

Paired T-Test Analysis	95% CI	P value
4209-02 vs. 4309-03	0.2201 to 0.7654	<0.0001
4209-02 vs. 4409-04	1.116 to 1.811	<0.0001
4209-02 vs. 4509-05	2.097 to 2.961	<0.0001
4209-02 vs. 4609-06	2.449 to 3.174	<0.0001
4309-03 vs. 4409-04	0.7215 to 1.221	<0.0001
4309-03 vs. 4509-05	1.658 to 2.415	<0.0001

4309-03 vs. 4609-06	1.934 to 2.704	<0.0001
4409-04 vs. 4509-05	0.7063 to 1.424	<0.0001
4409-04 vs. 4609-06	0.9640 to 1.732	<0.0001
4509-05 vs. 4609-06	-0.01758 to 0.5828	0.0738

Table 1: Significant differences between the airfoils with different camber positions
**CI-Confidence Interval*

Discussion

The results show that as the camber of a wing moves forward the amount of lift produced at any angle of attack increases along with the maximum amount of lift produced. The stall angle however decreases as the camber moves forward.

A previous study that analyzed the camber position but that did not alter the thickness position also saw an increase in the maximum lift coefficient as the camber moves forward, but did not show a trend in the stall angle[7]. Therefore, based on this study and the previous one, it seems that moving the camber position forward increases the amount of lift produced but does not aid the stall angle (this study shows that it decreases the stall angle). Moving the wing camber (along with the thickness position) rearward on an airfoil may provide stall resistant characteristics by increasing the stall angle but it comes with a trade off in terms of decreased lift.

The limitations of this experiment are that it does not compare all thickness and camber combinations but rather matches them at the same distance from the leading edge of the wing. Therefore, different combinations may provide better stalling characteristics.

Methods

Producing the airfoils

Five airfoils were designed with the Airfoil Design application. Each airfoil is represented with a modified four-digit NACA number. To change the camber both the camber position and the thickness position were changed, the second and last digits. Each airfoil was given a chord length of 6cm and a span of 8cm. The airfoils were developed as CAD models and three-dimensionally printed.

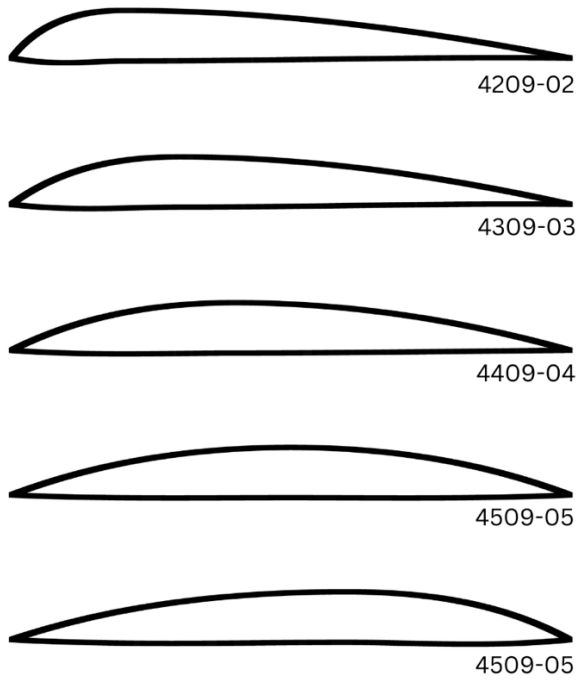

Figure 3: Airfoil NACA numbers.

Obtaining lift values

To obtain lift values, each airfoil was mounted to a scale with an angle gauge so that the angle of attack could be altered. As the wind tunnel fan was on, their produced lift forces were measured on the scale. For each airfoil, lift was measured in grams from 0 degrees to 90 degrees increasing by 2-degree increments. Three trials were recorded for each lift value of each angle and then averaged. When comparing airfoil lift data, a 5% error rate was accepted (p-value of 0.05). 10 measurements were taken for the speed of the fan at the position of the airfoils and averaged. Then, the lift coefficients were calculated using equation 1.

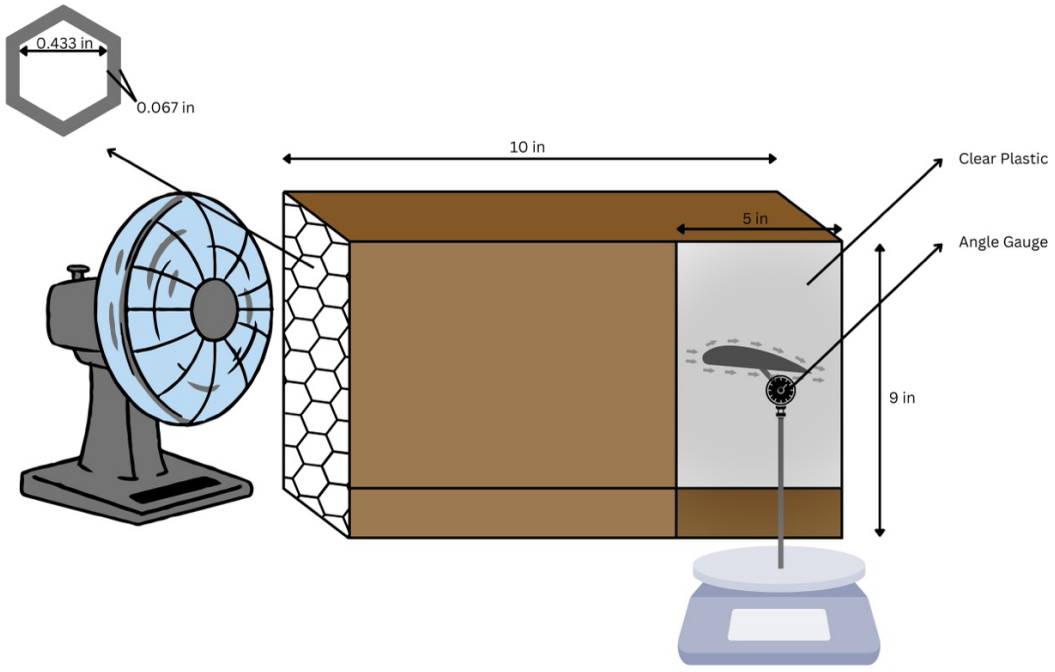

Figure 4: Wind tunnel diagram.

References

1. N. D. Katopodes. *Free-Surface Flow Environmental Fluid Mechanics*. https://www.sciencedirect.com/topics/engineering/coanda-effect (2019).
2. J. G. Leishman. Stalling & Spinning. *Embry-Riddle Aeronautical University.* https://eaglepubs.erau.edu/introductiontoaerospaceflightvehicles/chapter/maximum-lift-stalling-spinning/ (2022).
3. T. Benson. Bernoulli and Newton. *NASA Glenn Research Center*. https://www.grc.nasa.gov/www/k-12/VirtualAero/BottleRocket/airplane/bernnew.html
4. M. E. Lyall, P. I. King, J. P. Clark, R. Sondergaard. Endwall loss reduction of high lift low pressure turbine airfoils using profile contouring: part I - airfoil design (2013).
5. M. S. Genç, K. Koca, H. H. Açikel. Investigation of pre-stall flow control on wind turbine blade airfoil using roughness element. *Elsevier* (2019).
6. J. Liu, R. Chen, Y. You, Z. Shi. Numerical investigation of dynamic stall suppression of rotor airfoil via improved co-flow jet (2021).
7. E. N. Jacobs, R. M. Pinkerton. Tests in the variable-density wind tunnel of related airfoils having the maximum camber unusually far forward (1936).
8. E. N. Jacobs, R. M. Pinkerton, H. Greenberg. Tests of related forward-camber airfoils in the variable-density wind tunnel (1937).
9. *Stanford*. https://web.stanford.edu/~cantwell/AA200_Course_Material/The%20NACA%20airfoil%20series.pdf
10. M. Dasilva. Lift equation. *NASA Glenn Research Center*. https://www1.grc.nasa.gov/beginners-guide-to-aeronautics/lift-equation-2/ (2023).

11. Jeff Scott. Lift Equation. https://aerospaceweb.org/question/aerodynamics/q0015b.shtml (2001).
12. Wing area. T. Benson. *NASA Glenn Research Center.* https://www.grc.nasa.gov/www/k-12/VirtualAero/BottleRocket/airplane/area.html